

# The local structures in liquid water

Cheng Yang,<sup>1</sup> Chuanbiao Zhang,<sup>2</sup> Fangfu Ye<sup>a,1</sup> and Xin Zhou<sup>b2</sup>

<sup>1</sup>*Institute of Physics, Chinese Academy of Sciences, Beijing 100190, China*

<sup>2</sup>*School of Physical Sciences, University of Chinese  
Academy of Sciences, Beijing 100049, China*

(Dated: November 21, 2016)

## Abstract

The local structure of liquid water is very important to understand the water anomalous properties. The liquid-liquid phase transition (LLPT) scenario can explain those anomalies correctly, which proposes that there are two structural forms, the high density liquid (HDL) and low density liquid (LDL), in liquid water. There is a coexistence line ending at a liquid-liquid critical point (LLCP) in the supercooled region between these two forms. We use several order parameters to analyse the inherent structure of liquid water from supercooled to normal temperature at ambient pressure. We find that there is a new type of local structure except the HDL and LDL. Molecules with new structure have highest local density and are surrounded by the HDL molecules. We also demonstrate that this new type of local structure exists not only in the inherent structure but also in the real structure.

---

<sup>a</sup> E-Mail: fye@iphy.ac.cn

<sup>b</sup> E-Mail: xzhou@ucas.ac.cn

## I. INTRODUCTION

Water is the most common substance on the earth and plays a core role in many physical, chemical and biological processes. But its unusual thermodynamic properties remain elusive. For example, the isothermal compressibility, isobaric heat capacity and the magnitude of thermal expansion coefficient, all are related to the fluctuation in liquid water, increasing sharply contrary to normal liquid upon cooling [1]. Many theories are proposed to explain these peculiar properties [2–4]. In 1992, Poole et al. [5] proposed the liquid-liquid phase transition (LLPT) scenario requiring a new critical point in supercooled region. Above the critical point, two different forms of liquid water, high-density liquid (HDL) and low-density liquid (LDL), were separated by a first-order phase transition line. In the supercritical region, the liquid water is a mixture of these two different kinds of local structure. This hypothesis has received many experimental and theoretical supports in the last decades [6–29].

The new critical point is below the homogeneous nucleation temperature in theory. The fast nucleation process will prevent the measurements on the structure of liquid water. However, many experiments have provided some evidences consistent with LLPT scenario. The decline of density was observed in supercooled region when combine liquid water in nanopores [7, 8]. But the correlation between the bulk and confined water is questioned for the influence of the pore wall [30]. In ambient conditions, the X-ray spectroscopy shows that the liquid water has two types of local structures [10, 12, 13]. Some anomalies in bulk supercooled water at negative pressure is found [15]. Recently, Sellberg and his co-workers [14] use ultrafast X-ray to probe the structure of water in micrometre-sized droplets below homogeneous ice nucleation temperature and find that the structure of liquid water in no man’s land exhibits stronger tetrahedral ordering. Though all the experiments shed a light on the critical phenomenon of liquid water, but the critical point is still unknown. Molecular dynamics simulation is an useful tool to study the LLC. The second critical point of TIP4P/2005 water model is located at  $P_c = 1350$  bar and  $T_c = 193$  K [19]. In the coexistence region, the free energy surface of liquid water shows two distinct minimum separated by the density [27]. An interfacial area separating two different liquid phases occurs soon when fix the density of system between these two liquid states [28]. In supercritical water, it’s difficult to distinguish this two different local structures in real trajectory, but it can be done in inherent structure obtained by quenching the instantaneous conformation into the

local minimum on the potential energy surface [18, 20, 21].

In this paper, we apply multiple order parameters to characterize the inherent structure of liquid water ranging from supercooled to ambient temperature at atmosphere pressure. We find that the HDL molecules will gather around a molecule with higher local density and less tetrahedral symmetry at all the temperatures. The proportion of molecules with this new local structure increases when heat the system. We also demonstrate that this new type local structure can also be extracted from the real trajectory at very low temperatures where the thermal fluctuation is small.

## II. METHOD

### A. simulation

All the simulations are performed in the isothermal-isobaric(NPT) ensemble using the molecular dynamics package LAMMPS [31] and GROMACS [32]. We employ three water models, TIP4P/2005 [33], TIP4P-Ew [34] and SPC/E [35] in this paper. The main analyses are based on the TIP4P/2005 model and the others provide the supports for the results. The simulations of TIP4P/2005 model contain 216 and 4000 molecules. The temperature of 216-molecule simulation ranges from 200K to 300K and the simulation time at different temperatures is various. The shortest run is 100ns at 300K and the total length at 200K is more than 1000ns. The 4000-molecule simulation runs at 230K for 20ns and 300K for 10ns. The TIP4P-Ew and SPC/E simulations both contain 1000 molecules and run at 300K for 20ns. The real structures are exported during simulation and minimized respectively with the conjugate gradient algorithm to obtain the inherent structures. The minimization can remove the vibrational component from thermodynamics properties of liquid water.

### B. local order parameters

Local structure index (LSI)  $I(i)$ . This index is used to characterize the gap between first and second shells of water molecule  $i$ . The high value of  $I(i)$  indicates that there are well defined shells of the considered molecule. While the low value implies the gap disappears, *i.e.*, the second shell collapses.  $I(i)$  is defined as follow [18, 20, 21]. For each molecule, sort the distance  $r_j$  between central molecule  $i$  and its neighbours  $j$  as  $r_1 < r_2 < r_3 \cdots < r_{n(i)} <$

$0.37\text{nm} < r_{n(i)+1}$ . Let  $\Delta(j, i) = r_{j+1} - r_j$  and  $\overline{\Delta(i)}$  denote the average of  $\Delta(j, i)$  over all molecules whose distances to the central molecule are less than  $0.37\text{nm}$ . Then,

$$I(i) = \frac{1}{n(i)} \sum_{j=1}^{n(i)} [\Delta(j, i) - \overline{\Delta(i)}]^2.$$

Distance of the fifth molecule  $r_5(i)$ . The distance between central molecule  $i$  and its fifth closest neighbour is denoted as  $r_5(i)$  [37]. In the well-separated shells, the first shell contains about four molecules, so the fifth nearest neighbour belongs to the second shell usually. But if the structure is distorted, the fifth neighbour will insert into the gap between the first and second shells to decrease the value of  $r_5(i)$ .

Tetrahedral parameter  $q(i)$ . The nearest four neighbours of molecule  $i$  in the first shell favour tetrahedral symmetry structure. The tetrahedral parameter  $q(i)$  is used to characterize the degree of this symmetry [38].  $q(i)$  is defined as

$$q(i) = 1 - \frac{3}{8} \sum_j^3 \sum_{k=j+1}^4 (\cos(\psi_{jk}) + \frac{1}{3}),$$

where the  $\psi_{jk}$  is the angle composed by center molecule  $i$  and its two neighbours  $j$  and  $k$ . The value of  $q(i)$  approaching to one implies that the local structure is in a geometry like ice. However, when  $q(i)$  is close to zero the local structure is disordered.

local density  $\rho(i)$ . We calculate the local density of molecule  $i$  via adopting the reciprocal of its occupied volume,  $\rho(i) = \frac{m}{v(i)}$ . Where  $m$  is the mass of a single water molecule.  $v(i)$  is the volume of Voronoi cell which is a convex polyhedron covering the central molecule  $i$ .

### III. RESULTS

#### A. A new type of local structure

In Fig.1(a) we show the probability distribution of LSI in inherent structure at different temperatures. Each curve exhibits a bimodal characteristic consistent with earlier study [21]. The minimum is between  $0.13$  and  $0.14 \text{ \AA}^2$  and separates the water molecules into HDL (low  $I$ ) and LDL (high  $I$ ). The inset shows the density of liquid water in real structure as a function of temperature. The density decreases sharply upon cooling after reaching the maximum value around  $280\text{K}$ . It implies the system has crossed the Widom line which is

the extension of liquid-liquid phase transition line beyond the critical point [19]. At high temperature, the HDL component dominates the liquid water, while at low temperature, the LDL does. Fig 1(b) shows the probability distributions of  $r_5$  in inherent structure at different temperatures. All the distributions are bimodal, too. The minimum is around  $3.0\text{\AA}$  and the left peak increases upon heating. The results of TIP4P-Ew and SPC/E model are shown in the inset, they also have two peaks. Now we will demonstrate that the bimodal distribution of  $r_5$  occurs not only in inherent structure but also in real structure. We abstract all the single-molecule trajectories in real structure at low temperature and calculate their probability distributions of  $r_5$ . In Fig.1(c) and Fig.1(d) we show all the single-molecule probability distributions at 200K and 210K respectively. The envelope curve of these distributions shows bimodal-peak pattern obviously at both temperatures.

In both  $I$  and  $r_5$  parameter space, all the distributions show a bimodal characteristic. In the following, we will discuss the relationship between parameter  $I$  and  $r_5$ . In Fig.2 we calculate the two-dimensional probability distributions of local structures in inherent structure at 300K. Fig.2(a) shows the  $I - r_5$  map. There are three peaks in this plane, which are named as  $s_1$ ,  $s_2$  and  $s_3$  marked on this figure. Fig.2(b) shows  $I - v$  map.  $v$  is the local volume of each molecule obtained through its Voronoi cell. There are two peaks separated by the minima of  $I$ . The volume of left peak is smaller than that of right peak, which is consistent with that the low-LSI is HDL and high-LSI is LDL. Consider (a) and (b) together, we can find that  $s_1$  and  $s_2$  molecules compose HDL and  $s_3$  is LDL. Fig.2(c) and Fig.2(d) show that the  $s_1$  molecules have the smallest local volume and lowest tetrahedral symmetry.

The minimizing potential energy process can remove the vibrational component from the simulation conformations [39]. Now we will discuss how local environment changes when quench the simulation conformation into the minimum on the potential energy surface. In Fig.3(a) shows the probability distributions of the number of H-bonds of different local structures in inherent structure at 300 K. Almost all  $s_1$  molecules have five H-bonds. Part of  $s_2$  molecules have four H-bonds and the others have three. The  $s_3$  molecules are most tetrahedral symmetrical for the majorities have four H-bonds. In real structure, we classify molecules according to their local environments in inherent structure. The corresponding probability distributions of H-bonds are shown in Fig.3(b). The relative position of distributions of different type local structures are invariable in the quenching process. Fig.3(c)

and (d) show the distributions of different local structures in parameter  $\rho$  and  $q$  space after quenching. The insets show the same curves obtained in real structure. The main properties of different type local structures are reserved during the minimization.

Base on above statistical results, we show the local structures of different types in inherent structure in Fig.4. The snapshot of  $s_1$  is shown in Fig.4(a). The center molecule is overcoordinated and has three acceptor and two donor hydrogen bonds. In Fig.4(b),(c) and (d) we show the schematic descriptions of three type local structures. The first shell of  $s_1$  molecules has five neighbours and the sixth neighbour is near the 0.37nm circle which is used as cut-off value in the calculation of LSI (see Fig.4(b)). Fig.4(c) shows the  $s_2$  molecule has four neighbours in the first shell. The fifth neighbour is between the first shell and 0.37nm circle which consistent with the picture of HDL in former work [1]. The local structure of  $s_3$  molecule is ice-like and the fifth neighbour is beyond the 0.37nm circle (see Fig.4(d)).

## B. Spatial correlation of different type local structures

Now we will discuss the spatial correlation of different type local structures in inherent structure. In Fig.5(a) and (b) we show the snapshots of liquid water at 230K and 300K. The red, white and green spheres represent the  $s_1, s_2$  and  $s_3$  molecules respectively. At both temperatures, the  $s_1$  molecules are dispersed in the whole space, while  $s_2$  and  $s_3$  molecules seem like to cluster with that in the same type. In order to confirm this phenomenon, we calculate the Oxygen-Oxygen (O-O) radial distribution functions for different types at 300K (see Fig.5(c)). The first peak increases through  $s_1$  to  $s_3$ , which implies that the clustering effect becomes more and more strong. The results are consistent with the impression we have got from the snapshots. Fig.5(d) shows  $s_1$ - $s_2$  ( $g_{12}$ ) and  $s_1$ - $s_3$  ( $g_{13}$ ) cross radial distribution functions at 300K. The first peak of  $g_{12}$  is much bigger than that of  $g_{13}$ , which implies that the number of  $s_2$  molecules are far more than  $s_3$  molecules in the first shell of  $s_1$  molecules. In consideration of the fact that  $s_1$  molecules are discrete, so the  $s_1$  molecule are almost surrounded by  $s_2$  molecules.

Let  $c_i$  denote the concentration of  $s_i$  molecules in the total system. The proportion of  $s_j$  molecules in the nearest four neighbours of  $s_i$  molecule is defined as  $o_{ij}$ . Temperature dependence of  $c_i$  and  $o_{ij}$  are shown in Fig.6. In Fig.6(a),  $c_1$  is smaller than  $o_{21}$  and bigger than  $o_{31}$  at all the temperatures, which implies  $s_2$  ( $s_3$ ) molecules will attract (repel)  $s_1$

molecules. Fig.6(b) shows  $c_2$  is smaller than  $o_{12}$  and bigger than  $o_{32}$  at all the temperatures. That is to say the molecules in  $s_1$  ( $s_3$ ) type will attract (repel) that in  $s_2$  type. And  $o_{12}$  is far bigger than  $o_{21}$  indicates molecules in  $s_1$  are surrounded by  $s_2$  molecules, which is consistent with the results of Fig.5. In Fig.6(c) we show that  $c_3$  is bigger than  $o_{13}$  and  $o_{23}$ , which represents that  $s_3$  molecules will repel both  $s_1$  and  $s_2$  molecules.

In Fig.7 we show the evolution of  $o_{i2}$ . The proportion of molecules remaining in the  $s_1$  type changes with time was shown in Fig.7(a). It decreases fast. The  $o_{12}$  of molecules remaining in  $s_1$  increases with time(see Fig.7(b)), which implies that more  $s_2$  molecules will get together in the first shell when the center molecule stay in  $s_1$  for longer time. In Fig.7(c) we show the time dependence of the proportion of molecules remaining in  $s_3$ . It decreases a little more slowly than that in  $s_1$ . The time dependence of  $o_{32}$  of molecules remaining in  $s_3$  was shown in Fig.7(d). It decreases with the time of center molecules stay in  $s_3$  for the repelling effect.

#### IV. CONCLUSION AND DISCUSSION

In this paper, we use multiple order parameters to describe the local structure of liquid water in inherent structure from 200K to 300K. We find that the local structure of water molecule has three types, the  $s_1$ ,  $s_2$  and  $s_3$ . The  $s_1$  molecule has five-coordinated neighbours in its first shell. However, the  $s_2$  molecule is the HDL with the fifth neighbours in the interval between first and second shell and  $s_3$  molecule is LDL with the fifth neighbour in the second shell. We also demonstrate that the  $s_1$  type local structure can be extracted from real structure at very low temperature where the thermal fluctuation is small. Then we analyse the spatial correlations of different types. Molecules in  $s_1$  type disperse in the whole space, but  $s_2$  and  $s_3$  molecules like to cluster with the same types. The  $s_1$  molecule are surrounded by the  $s_2$  molecules and the number of  $s_2$  molecules in the first shell will increase with the time of center molecule stay in  $s_1$  type. The  $s_1$  molecule is like a “condensation nucleus” of  $s_2$  molecules.

---

[1] P. G. Debenedetti, Journal of Physics: Condensed Matter **15**, R1669 (2003).

[2] R. J. Speedy, The Journal of Physical Chemistry **86**, 982 (1982).

- [3] C. A. Angell, *Science* **319**, 582 (2008).
- [4] S. Sastry, P. G. Debenedetti, F. Sciortino, and H. E. Stanley, *Physical Review E* **53**, 6144 (1996).
- [5] P. H. Poole, F. Sciortino, U. Essmann, and H. E. Stanley, *Nature* **360**, 324 (1992).
- [6] P. Wernet, D. Nordlund, U. Bergmann, M. Cavalleri, M. Odelius, H. Ogasawara, L. Näslund, T. Hirsch, L. Ojamäe, P. Glatzel, *et al.*, *Science* **304**, 995 (2004).
- [7] D. Liu, Y. Zhang, C.-C. Chen, C.-Y. Mou, P. H. Poole, and S.-H. Chen, *Proceedings of the National Academy of Sciences* **104**, 9570 (2007).
- [8] F. Mallamace, C. Branca, M. Broccio, C. Corsaro, C.-Y. Mou, and S.-H. Chen, *Proceedings of the National Academy of Sciences* **104**, 18387 (2007).
- [9] T. Tokushima, Y. Harada, O. Takahashi, Y. Senba, H. Ohashi, L. G. Pettersson, A. Nilsson, and S. Shin, *Chemical Physics Letters* **460**, 387 (2008).
- [10] C. Huang, K. T. Wikfeldt, T. Tokushima, D. Nordlund, Y. Harada, U. Bergmann, M. Niebuhr, T. Weiss, Y. Horikawa, M. Leetmaa, *et al.*, *Proceedings of the National Academy of Sciences* **106**, 15214 (2009).
- [11] M. Paolantoni, N. F. Lago, M. Albertí, and A. Lagana, *The Journal of Physical Chemistry A* **113**, 15100 (2009).
- [12] A. Nilsson and L. G. Pettersson, *Chemical Physics* **389**, 1 (2011).
- [13] A. Nilsson, C. Huang, and L. G. Pettersson, *Journal of Molecular Liquids* **176**, 2 (2012).
- [14] J. A. Sellberg, C. Huang, T. McQueen, N. Loh, H. Laksmono, D. Schlesinger, R. Sierra, D. Nordlund, C. Hampton, D. Starodub, *et al.*, *Nature* **510**, 381 (2014).
- [15] G. Pallares, M. E. M. Azouzi, M. A. González, J. L. Aragones, J. L. Abascal, C. Valeriani, and F. Caupin, *Proceedings of the National Academy of Sciences* **111**, 7936 (2014).
- [16] L. Xu, P. Kumar, S. V. Buldyrev, S.-H. Chen, P. H. Poole, F. Sciortino, and H. E. Stanley, *Proceedings of the National Academy of Sciences of the United States of America* **102**, 16558 (2005).
- [17] M. Matsumoto, A. Baba, and I. Ohmine, *The Journal of chemical physics* **127**, 134504 (2007).
- [18] G. Appignanesi, J. R. Fris, and F. Sciortino, *The European Physical Journal E* **29**, 305 (2009).
- [19] J. L. Abascal and C. Vega, *The Journal of chemical physics* **133**, 234502 (2010).
- [20] S. Accordino, J. R. Fris, F. Sciortino, and G. Appignanesi, *The European Physical Journal E* **34**, 1 (2011).



- [21] K. Wikfeldt, A. Nilsson, and L. G. Pettersson, *Physical Chemistry Chemical Physics* **13**, 19918 (2011).
- [22] T. Kesselring, G. Franzese, S. Buldyrev, H. Herrmann, and H. E. Stanley, *Scientific reports* **2** (2012).
- [23] Y. Liu, J. C. Palmer, A. Z. Panagiotopoulos, and P. G. Debenedetti, *The Journal of chemical physics* **137**, 214505 (2012).
- [24] Y. Li, J. Li, and F. Wang, *Proceedings of the National Academy of Sciences* **110**, 12209 (2013).
- [25] N. Giovambattista, *Liquid Polymorphism*, Volume 152 , 113 (2013).
- [26] P. H. Poole, R. K. Bowles, I. Saika-Voivod, and F. Sciortino, *The Journal of chemical physics* **138**, 034505 (2013).
- [27] J. C. Palmer, F. Martelli, Y. Liu, R. Car, A. Z. Panagiotopoulos, and P. G. Debenedetti, *Nature* **510**, 385 (2014).
- [28] T. Yagasaki, M. Matsumoto, and H. Tanaka, *Physical Review E* **89**, 020301 (2014).
- [29] J. Russo and H. Tanaka, *Nature communications* **5** (2014).
- [30] R. Mancinelli, S. Imberti, A. Soper, K. Liu, C. Mou, F. Bruni, and M. A. Ricci, *The Journal of Physical Chemistry B* **113**, 16169 (2009).
- [31] See <http://lammps.sandia.gov/> for information about the LAMMPS molecular dynamics simulator..
- [32] See <http://www.gromacs.org/> for information about the GROMACS molecular dynamics simulator..
- [33] J. L. Abascal and C. Vega, *The Journal of chemical physics* **123**, 234505 (2005).
- [34] H. W. Horn, W. C. Swope, J. W. Pitera, J. D. Madura, T. J. Dick, G. L. Hura, and T. Head-Gordon, *The Journal of chemical physics* **120**, 9665 (2004).
- [35] H. Berendsen, J. Grigera, and T. Straatsma, *Journal of Physical Chemistry* **91**, 6269 (1987).
- [36] C. Vega and J. L. Abascal, *Physical Chemistry Chemical Physics* **13**, 19663 (2011).
- [37] M. J. Cuthbertson and P. H. Poole, *Physical review letters* **106**, 115706 (2011).
- [38] J. R. Errington and P. G. Debenedetti, *Nature* **409**, 318 (2001).
- [39] P. G. Debenedetti and F. H. Stillinger, *Nature* **410**, 259 (2001).

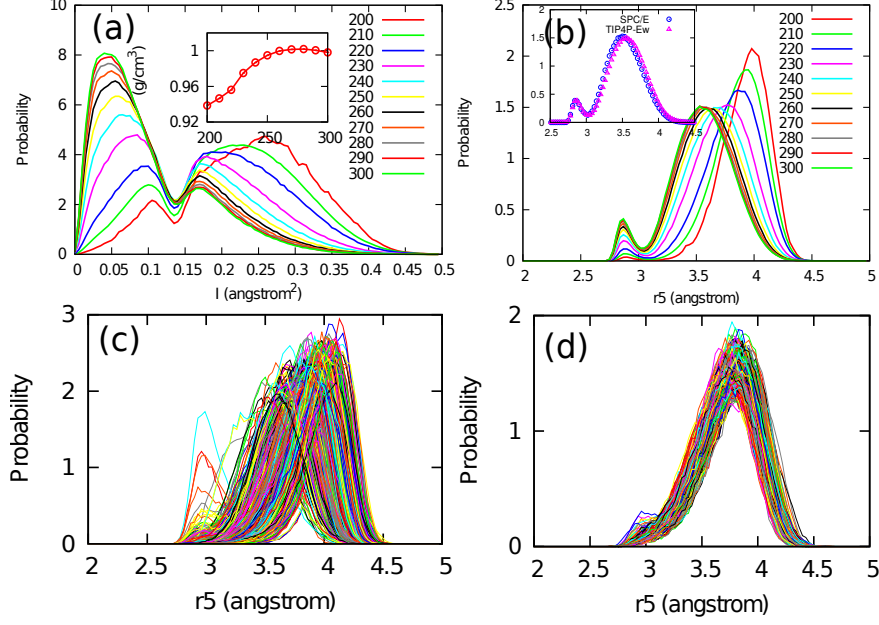


FIG. 1. (a) The probability distribution of LSI of 216-molecule simulations in inherent structure at different temperatures. The inset shows the corresponding density of liquid water in real structure changing with temperature. (b) The distribution of  $r_5$  of 216-molecule simulations in inherent structure at different temperatures. All the curves have a minimum around 3  $\text{\AA}$ . The results of TIP4P-Ew and SPC/E model in inherent structure at 300 K are shown in the inset. (c) and (d) The probability distributions of  $r_5$  of single-molecule trajectories in real structure at 200 K and 210 K respectively. The envelope curve of these distributions shows bimodal-peak pattern at both temperatures.

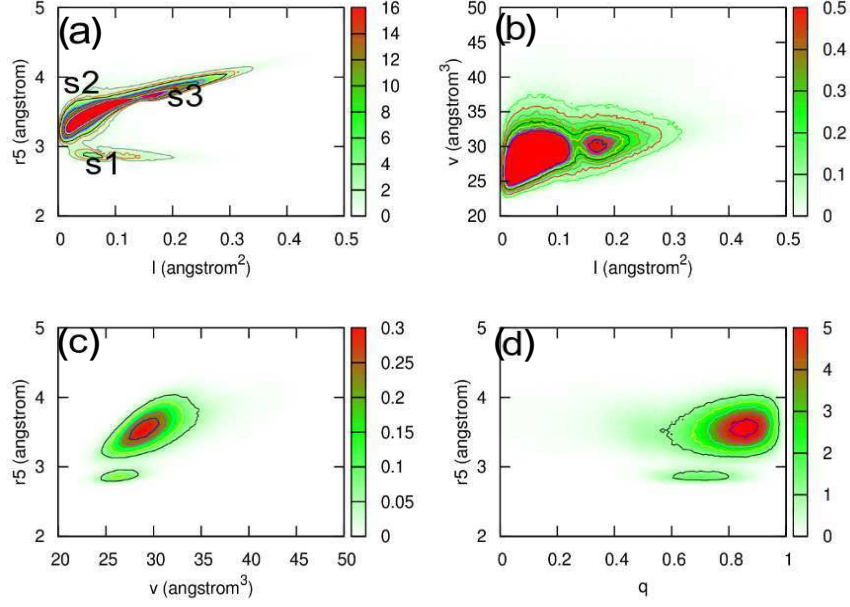


FIG. 2. Two-dimensional distributions of 216-molecule simulations in inherent structure at 300 K. (a)  $I - r_5$  map. The water's local structures can be classified into three types,  $s_1$ ,  $s_2$  and  $s_3$ , according to the shape of the distribution. (b)  $I - v$  map. There is a clear separation between LDL (high- $I$ ) and HDL (low- $I$ ). Comparing (a) and (b), we can see that  $s_1$  and  $s_2$  molecules form HDL and  $s_3$  molecules corresponding to LDL. (c)  $v - r_5$  map. (d)  $q - r_5$  map. The local volume  $v$  and tetrahedral parameter  $q$  of  $s_1$  molecules are smaller than that of  $s_2$  and  $s_3$  molecules.

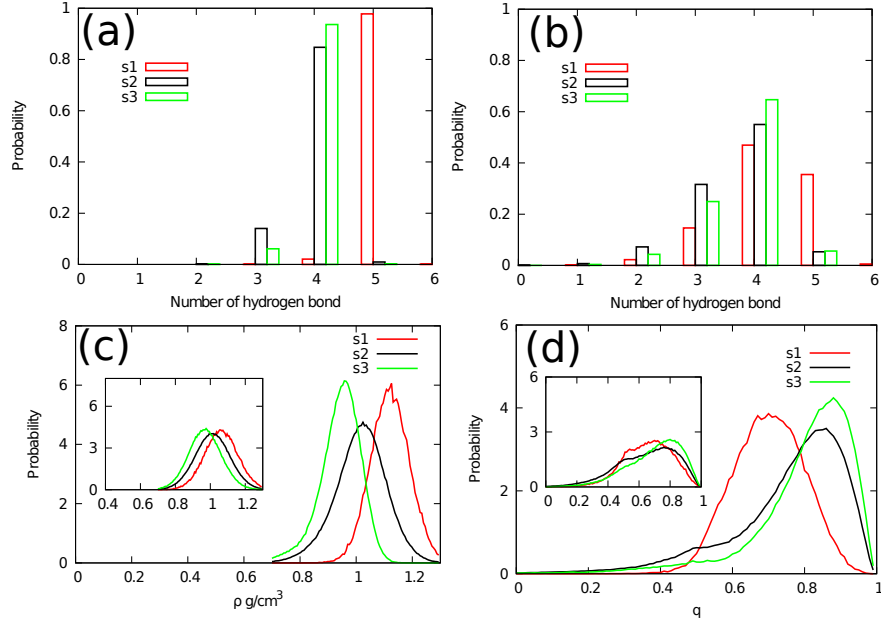


FIG. 3. The relationship between inherent structure and real structure in 4000-molecule simulations. (a) In inherent structure, the distributions of the number of H-bonds of molecules in different types. (b) In real structure, the corresponding distributions of the number of H-bonds. (c) and (d) Distributions of local density  $\rho$  and tetrahedral symmetry  $q$  of different type local structures in inherent structure. The insets show the same curves obtained in real structure.

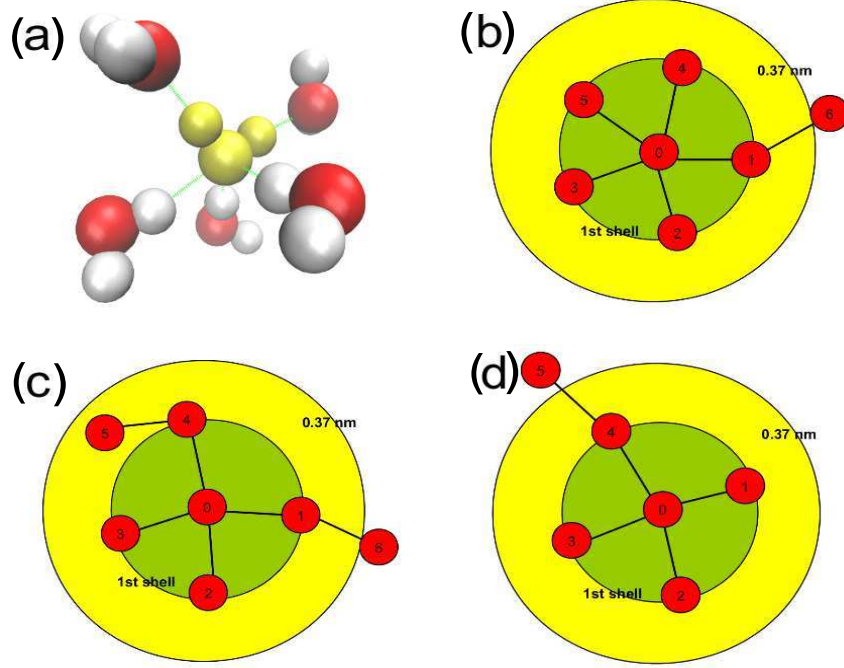


FIG. 4. (a) The snapshot of  $s_1$  in inherent structure. The center molecule has three acceptor and two donor hydrogen bonds. (b), (c) and (d) show the schematic descriptions of different local structures in inherent structure. (b)  $s_1$  molecule has five neighbours in the first shell. (c)  $s_2$  molecule has four neighbours in the first shell. The fifth neighbour is between the first shell and 0.37nm circle. (d)  $s_3$  molecule has four neighbours in first shell. The fifth neighbour is beyond the 0.37nm circle obviously.

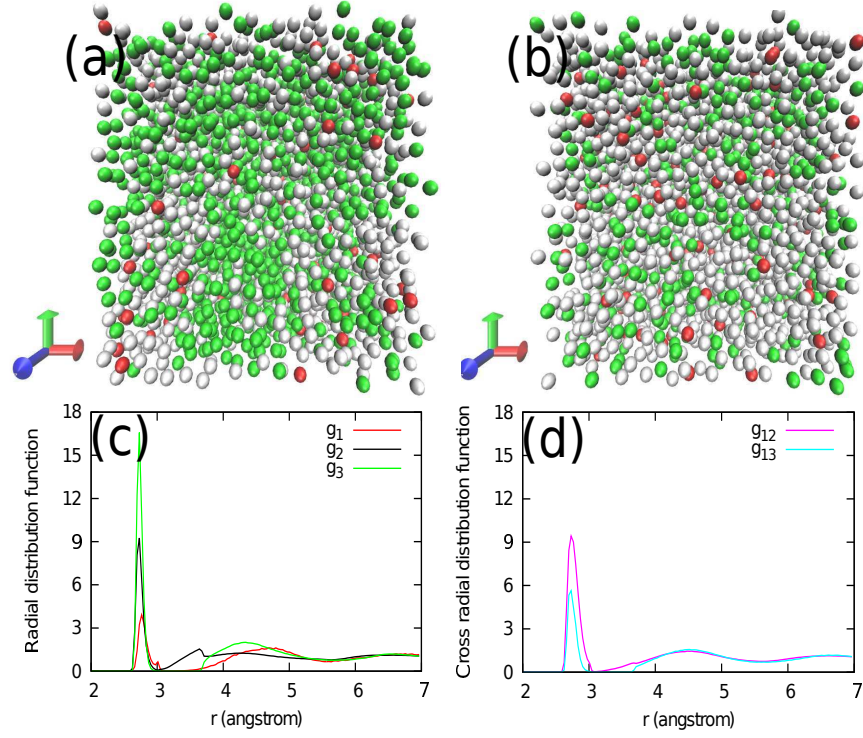


FIG. 5. Spatial relation of different type local structures in inherent structure of 4000-molecule simulations. (a) and (b) show the snapshots of liquid water at 230K and 300K. The red, white and green spheres represent the  $s_1, s_2$  and  $s_3$  molecules respectively. (c) The O-O radial distribution functions of different types at 300K. (d) The  $s_1$ - $s_2$  (magenta) and  $s_1$ - $s_3$  (cyan) radial distribution functions at 300K.

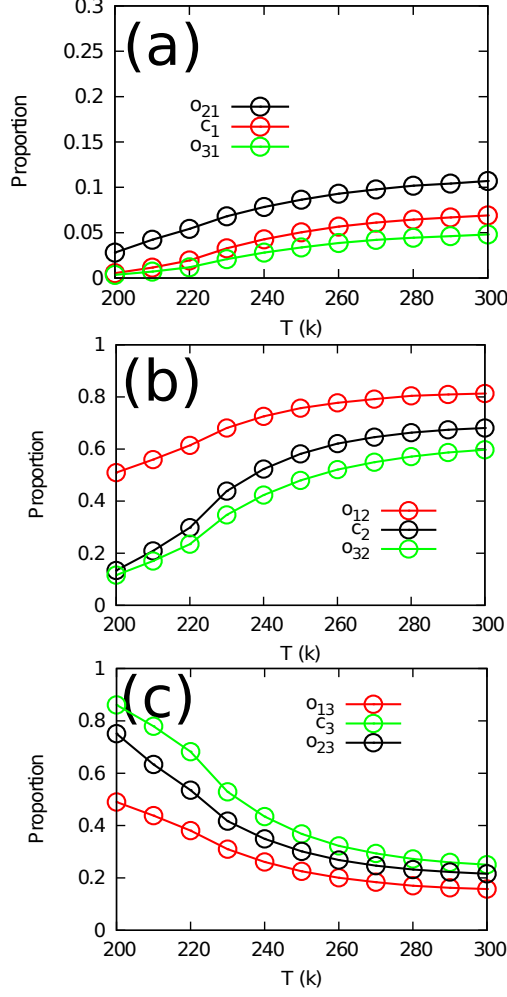


FIG. 6. Compare  $c_j$  and  $o_{ij}$  in inherent structure of 216-molecule simulations. (a)  $c_1$  is smaller than  $o_{21}$  and bigger than  $o_{31}$  implies  $s_2$  ( $s_3$ ) molecules will attract (repel)  $s_1$  molecules. (b)  $c_2$  is smaller than  $o_{12}$  and bigger than  $o_{32}$  shows that the  $s_1$  ( $s_3$ ) molecules will attract (repel)  $s_2$  molecules.  $o_{12}$  is far bigger than  $o_{21}$  indicates  $s_1$  molecules are covered by  $s_2$  molecules. (c)  $c_3$  is bigger than  $o_{13}$  and  $o_{23}$  represents  $s_3$  molecules repel both  $s_1$  and  $s_2$  molecules.

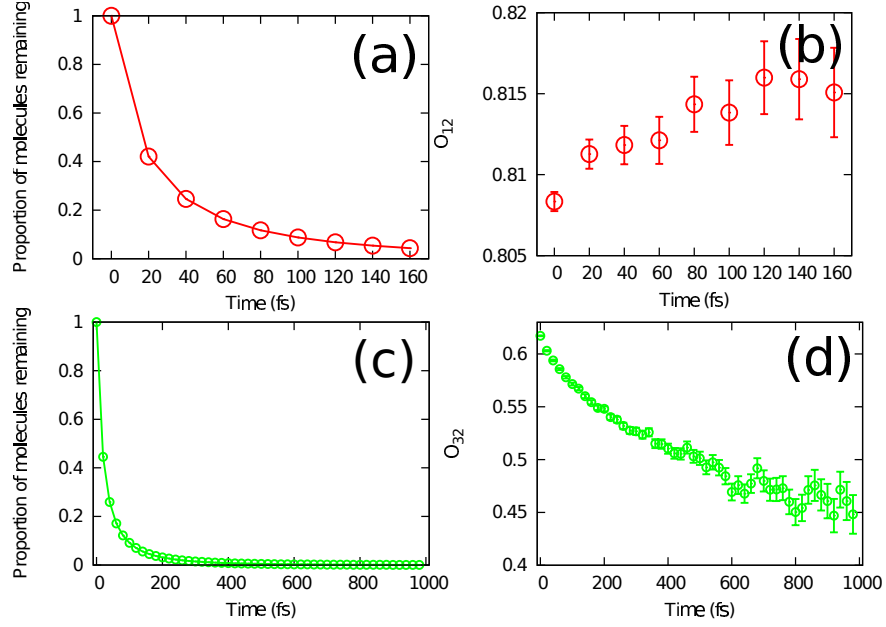


FIG. 7. Some properties of local structure change with time in inherent structure of 4000-molecule simulations at 300K. (a) The proportion of molecules remaining in  $s_1$  type changes with time. (b)  $o_{12}$  of molecules remaining in  $s_1$  type changes with time. (c) Time dependence of the proportion of molecules remaining in  $s_3$  type. (d) Time dependence of  $o_{32}$  of molecules remaining in  $s_3$  type.